Dynamic Stall Analysis in Light of Recent Numerical and Experimental Results

Lars E. Ericsson* and J. Peter Reding†
Lockheed Missiles & Space Company, Inc., Sunnyvale, Calif.

An earlier developed engineering analysis of dynamic stall is reviewed in light of recent numerical and experimental results. It is found that the concept of equivalence between boundary-layer improvement due to pitch-rate-induced effects and increasing Reynolds number is supported by the available numerical and experimental results. The existence of the postulated plunging-induced improvement of the boundary layer and associated delay of stall, the controversial "leading-edge jet" effect, is indicated by oscillatory stall data for different oscillation centers and by the measured negative aerodynamic damping for plunging oscillations in the stall region. More work is needed before the dynamic stall characteristics can be predicted for high frequencies. Until then, the present technique offers a reliable means for prediction of low-frequency ($\bar{\omega}<0.5$) dynamic stall characteristics from static experimental data.

Nomenclature

c = chord length
F,G = real and imaginary parts of the Theodorsen function
K_a = dynamic overshoot coefficient, Eq. (6)
k = reduced frequency, $2k=\bar{\omega}$
l = section lift, coefficient $c_l = l/(\rho_\infty U_\infty^2/2)c$
M = Mach number
m_p = section pitching moment, coefficient $c_m = m_p/(\rho_\infty U_\infty{}^2/2)c^2$
n = section normal force, coefficient $c_n = n/(\rho_\infty U_\infty^2/2)c$
p = static pressure, coefficient $C_p = (p-p_\infty)/(\rho_\infty U_\infty^2/2)$
Re = Reynolds number
t = time
U = velocity
x = chordwise distance from the leading edge
z = translatory coordinate, positive downward
α = angle of attack
α_0 = trim angle of attack
Δ = increment
ζ = dimensionless translatory displacement, $\zeta = -(z-z_{CG})/c$
θ = angle-of-attack perturbation
ξ,X = dimensionless x-coordinates, $\xi=x/c$, $X=2\xi-1$
ξ_{CG},a = center of oscillation, $\xi_{CG}=(a+1)/2$
ρ = air density
σ = pitch-rate-induced camber angle, $\sigma=\nu_{TE}-\nu_{LE}$
ν = camber line slope
ϕ = wake lag, Eq. (9)
ϕ_s = stall-induced additional phase lag, Eq. (9)
$\omega,\bar{\omega}$ = oscillation frequency, $\bar{\omega}=\omega c/U_\infty$

Subscripts

a = accelerated flow-induced equivalent time lag
AM = apparent mass
CG = center of gravity
c = convection
crit = critical
dyn = dynamic
e = boundary-layer edge conditions
LE = leading edge
max = maximum
r = reattachment
sp = separation point
w = wake and wall
$1,2$ = numbering subscript
∞ = undisturbed flow

Superscripts

i = induced and inducing, e.g., α^i = separation-inducing angle of attack. Eq. (9)
$*$ = complex variable, e.g., $\theta^* = \Delta\theta \exp(i\omega t)$

Differential symbols

$\dot{\alpha}$ = $\partial\alpha/\partial t$
$\ddot{\theta}$ = $\partial^2\theta/\partial t^2$
$c_{l\alpha}$ = $\partial c_l/\partial\alpha$

Presented as Paper 75-26 at the AIAA 13th Aerospace Sciences Meeting, Pasadena, Calif., Jan. 20-22, 1975; submitted Feb. 19, 1975; revision received July 2, 1975.

Index categories: Nonsteady Aerodynamics; Aircraft Aerodynamics (including Component Aerodynamics).

*Consulting Engineer. Associate Fellow AIAA.
†Research Specialist. Member AIAA.

Introduction

MANY years ago, Halfman et al.[1] outlined practical means for prediction of dynamic stall characteristics and set a precedence that has been followed by subsequent dynamic stall investigators.[2-4] This dynamic simulation technique works well as long as full-scale conditions really have been simulated. However, the reduced frequency usually cannot be simulated without violating the Reynolds and Mach number simulation necessary for simulation of true separated flow characteristics.[5] In addition, the so-called "two-dimensional" test data often are contaminated by tunnel wall or end-plate interference effects[5-7] Some years ago, the present authors developed a technique for prediction of dynamic stall characteristics from static airfoil section data.[8,9] The technique was quite successful in predicting experimental dynamic stall characteristics as long as the reduced frequencies were not high ($\bar{\omega}<0.5$). The advantages of this alternative to dynamic simulation a la Halfman et al.[1-4] are obvious; if the needed static data do not exist already, they are easy and relatively inexpensive to obtain, and both Reynolds number and Mach number effects can be investigated to provide the means for extrapolation to full-scale conditions.

The technique is semiempirical and uses dynamic experimental data to determine certain critical proportionality constants for the effects of pitch amplitude and frequency on the dynamic stall characteristics. The dynamic overshoot of

static stall is considered to be a completely viscous phenomenon. The inviscid unsteady flow effects are assumed to remain the same as for attached flow and are represented by a bilinear constant time lag/constant phase lag approximation[8] of the Karman-Sears vortex wake lag effect.[10] Physical flow concepts are introduced to explain the observed pitch rate effects on the dynamic overshoot of static stall. The $c_{l\max}$ overshoot is postulated to be the result of dynamic improvements of the boundary-layer characteristics, an effect that is assumed to be similar to that obtained by increasing the Reynolds number (in a static test) and, therefore, cannot exceed the "infinite Reynolds number limit." One source for this dynamic improvement of the boundary layer is the pressure-gradient-time-history effect on the boundary-layer development up to the separation point. As this effect would disappear in the case of the plunging airfoil, another additional source has to exist. Hence, the concept of the dynamic "leading-edge wall jet" or the "rolling leading edge" is introduced.[9,11]

Although some of the concepts introduced were accepted readily, others were more controversial. Since our original work,[8,9] further pertinent results have been published which throw new light on the subject. This paper analyzes these new data to determine the impact on our original analysis.[8,9] It is found that many of our basic assumptions are supported by recent numerical and experimental results, but it also is found that modifications are needed before satisfactory prediction of dynamic stall characteristics will be possible, especially at high frequencies and/or large amplitudes.

Engineering Analysis of Dynamic Stall

In order to be successful, any theory or computational technique for unsteady airfoil stall must account for two (anomalous) facts discovered by Halfman et al.[1]: 1) There is, in the dynamic case, a large overshoot of static $c_{l\max}$ (and associated c_m characteristics); and 2) pitch oscillation of an already stalled airfoil can re-establish attached flow over part of the oscillation cycle even when the minimum instantaneous angle of attack during the oscillation is larger than the static stall angle (α_s). In our engineering analysis,[8,9,11] we have postulated that these effects are caused by dynamic improvements of the boundary layer. The proposed viscous flow concepts are as follows: 1) boundary-layer improvement due to pitch-rate-induced upstream pressure gradient relief; 2) boundary-layer improvement caused by the leading-edge plunging, the so-called "leading-edge jet" effect; and 3) the upper boundary for dynamic improvement of the boundary layer is the static infinite Reynolds number limit.

In addition to this dynamic lift overshoot, with associated overshoot of static stall angle ($\Delta\alpha_s$), there is a pure time lag effect ($\Delta\alpha$), which has three contributions: 1) the Karman-Sears circulation lag $\Delta\alpha_w$, 2) boundary-layer convection lag $\Delta\alpha_c$, and 3) moving separation point delay $\Delta\alpha_{sp}$. The first is an inviscid effect, and the other two are of viscous origin.

In the following sections, it is recapitulated briefly how the foregoing flow concepts are used in our engineering analysis[8,9,11] to generate dynamic stall characteristics using static leading-edge stall data as an input.‡

Rampwise α-Change

When study the characteristics of unsteady airfoil stall, it is instructive to start with the simple case of rampwise change of angle of attack[9,11] (see Fig. 1). The dynamic overshoot of static stall has two components: $\Delta\alpha$ and $\Delta\alpha_s$. The component $\Delta\alpha$ is purely a lag effect and simply shifts the lift curve to higher α with no effect on $c_{l\max}$. The second component $\Delta\alpha_s$, however, produces a large overshoot $\Delta c_{L\max}$ over static $c_{l\max}$. On the pitching airfoil, the lift lags the instantaneous angle of attack owing to the time lag in the circulation buildup. For a thin airfoil at low angles of attack, this circulation lag has been defined by von Karman and Sears.[10] Using the lifting line representation, this circulation lag can be approximated by a constant time lag for rampwise α-change[8]

$$\Delta\alpha_w = \xi_w c\dot{\alpha}/U_\infty \tag{1}$$

where $\xi_w = 1.5$.

In the attached flow region ($\alpha < \alpha_s$), the experimental results[12] seem to indicate a lesser $\Delta\alpha$ than is predicted theoretically. However, the difference is not a $\Delta\alpha$ effect but is caused by the c_l increase through attached-flow-type apparent mass and pitch-rate-induced camber effects.[11] This c_l increase is completely negligible compared to the measured large overshoot of static $c_{l\max}$ (Fig. 1). Carta's proposed inviscid flow mechanism for dynamic stall overshoot[13] is really only this attached flow effect,[11] as is shown mathematically in the Appendix. In our engineering analysis,[8,9,11] we have postulated two mechanisms for the dynamic improvements of the boundary layer which can cause the observed $c_{l\max}$ overshoot. One such effect is the "accelerated flow" or "pressure gradient time history" effect. The nonstationary Bernouilli equation gives[8]

$$dp_e/d\xi = (\partial p_e/\partial\xi)_{\dot{\alpha}=0} + (\partial p_e/\partial\alpha)(c\dot{\alpha}/U_e) \tag{2}$$

That is, the local pressure gradient is less in the dynamic case than in the static case (at the same α) by the amount $-(\partial p_e/\partial\alpha)(c\dot{\alpha}/U_e)$. Thus, the boundary layer at separation has in the unsteady case a more favorable upstream time history. As a result, the boundary layer is improved and can stand a higher (critical) pressure gradient before separating. It has been shown by Shamroth and McDonald[14] that the quasi-steady pressure distribution prescribed by Eq. (2) gives the full unsteady boundary-layer characteristics for frequencies and pitch rates as high as $\bar{\omega}=2.0$ and $c\dot{\alpha}/U_\infty = 0.20$, respectively. As a result of the boundary-layer improvement, the static stall angle can be exceeded by an amount $\Delta\alpha_{sl}$, giving a corresponding overshoot of static $c_{l\max}$

$$> c_{l\max} = c_{l\alpha}\Delta\alpha_{s_l} \tag{3}$$

$$\Delta\alpha_{sl} = K_{al}\frac{c\dot{\alpha}}{U_\infty}\ ;$$

$$K_{al} = \frac{\{\partial/[\partial c\dot{\alpha}/U_\infty)]\}(\partial p_e/\delta\xi)_{\text{crit}}}{(\partial/\partial\alpha)(\partial p_e/\delta\xi)_{\dot{\alpha}=0}} \tag{4}$$

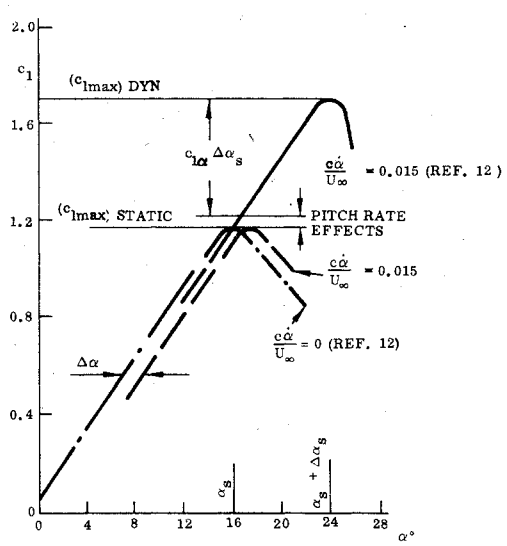

Fig. 1 Composition of α-ramp overshoot of static $c_{l\max}$.

‡Unless stated otherwise, only leading-edge-type stall is considered.

A Karman-Pohlhausen type of analysis[15] using this quasi-steady pressure distribution could give a measure of the boundary-layer time history effect with associated improvement of the shape parameter and decrease of the boundary-layer thickness, as was suggested in Refs. 9 and 11. In the numerical analysis performed by Scruggs et al.,[16] this thinning of the unsteady boundary layer is computed.

The other postulated mechanism for dynamic overshoot of static $c_{l\max}$ is the so-called "leading-edge jet" effect described in detail in Refs. 9 and 11. As the airfoil leading edge moves upward, the boundary layer is strengthened and stall delayed due to the vastly different tangential wall velocities between the leading edge and the top of the airfoil a short distance downstream. The boundary layer is accelerated by the rapidly moving leading edge and has an excess velocity when it "rounds the shoulder" to the slower-moving wall on the top of the airfoil. Thus, the boundary layer has a fuller profile and is therefore more difficult to separate.§ On the downstroke, the effect is the opposite, promoting separation. Wallis et al.[17-19] have shown that it is possible to trip the boundary layer, thereby eliminating the laminar bubble present for leading-edge stall, when applying blowing or distributed roughness between stagnation and separation points. Only minute amounts of blowing were required. Thus, there are reasons to expect that the "leading-edge jet effect" could contribute to $\Delta\alpha_s$ as much as, or more than, the pressure gradient-time history effect discussed earlier [Eq. (3)]. It is shown in Refs. 9 and 11 how this contribution $\Delta\alpha_{s2}$ would in a first approximation be proportional to the leading-edge plunging velocity $\dot{z}_{LE}$, That is

$$\Delta\alpha_{s2} = -K_{a2}(\dot{z}_{LE}/U_\infty) \tag{5}$$

For the airfoil pitching around ξ_{CG}, one obtains[9,11]

$$\Delta\alpha_s = K_a c\dot{\alpha}/U_\infty, K_a = K_{a1} + K_{a2}\xi_{CG} \tag{6}$$

These two mechanisms [Eqs. (3) and (5)] are straightforward and have the following important characteristics: 1) the effects are reversible, i.e., the effects are opposite on the "downstroke" to what they are on the "upstroke"; and 2) the effects are proportional to the dimensionless pitch and plunging rates, $c\dot{\alpha}/U_\infty$ and $\dot{z}_{LE}/U_\infty$, respectively. It will be shown later that $K_{a2} \approx 2K_{a1}$. Thus, our value $K_a = 3.0$ used for oscillations around $\xi_{CG} = 0.25$ corresponds to $K_{a1} = 2.0$ and $K_{a2} = 4.0$.

We have assumed in our analysis[9,11] that the improvement of the boundary layer through these two dynamic mechanisms is similar to the improvement obtained by increasing the Reynolds number. It therefore cannot exceed the infinite Reynolds number limit. Wallis et al.[17-19] have demonstrated the similarity between wall-jet induced boundary-layer profile change and that due to increased Reynolds number. Using static $c_{l\max}$ variation with Reynolds number [21,22] together with the measured dynamic overshoot[12,23] of static $c_{l\max}$, it was determined that the infinite Reynolds number limit for dynamic improvements was reached when $c\dot{\alpha}/U_\infty > 0.02$.[9,11] Likewise, on the "downstroke" the lift reduction is limited by c_l for $Re \to 0$.

Deep Stall Characteristics

The pitch-up data obtained by Ham and Garelick[3] show that, not only is there a dynamic overshoot of static $c_{l\max}$, but also the deep stall lift is substantially higher than in stationary flow. Static data[7,9,25] indicate that the airfoil has an early poststall region in which the separation point still is moving forward with increasing α. Thus the lift experiences a gradual decrease toward the fully stalled level[26] after the initial drop at stall. This transitory early poststall region can be extended to higher angles of attack for an airfoil in pitch-up motion. Moore[27] describes a mechanism that can generate this dynamic overshoot of the deep stall lift. When the separation point moves upstream, the boundary layer, ready to separate, "sees" a downstream moving wall, and the separation is deleyed¶ Thus, the separation point will lag its static position due to this moving wall effect, and a corresponding overshoot of the angle of attack will occur. For linear dependence, $\Delta\alpha_{sp}$ is

$$\Delta\alpha_{sp} = \xi_{sp}(c\dot{\alpha}/U_\infty) \tag{7}$$

The time lag parameter ξ_{sp} is defined as[9,11]

$$\xi_{sp} = \partial\xi_s/[\partial(U_w/U_\infty)] \tag{8}$$

From the rotating cylinder data obtained by Brady and Ludwig,[32] who used a shroud to impose an airfoil-like pressure distribution, we obtained the value $\xi_{sp} = 3.0$ by assuming that leading-edge stall is equivalent to the separation on the cylinder at subcritical Reynolds numbers.[9,11]

Oscillatory αChange

In the case of oscillatory α-change, the dynamic stall process is much more complicated than is the α-ramp case just discussed. It was shown in Ref. 8 how the Karman-Sears wake lag can be approximated by the constant time lag effect only as long as the reduced frequency is low, $\bar{\omega} < 0.16$. At higher frequency, a constant phase lag is the best approximation. Thus, for harmonic oscillations in pitch around α_0, e.g., $\alpha(t) = \alpha_0 + \Delta\theta \sin\omega t$, the generalized angle of attack, which determines when separation occurs, can be expressed as follows, representing the time history effects by descrete time lags

$$\alpha^i(t) = \alpha_0 + \Delta\theta \sin(\omega t - \phi - \phi_s) \tag{9a}$$

$$\phi = \begin{cases} \xi_w\bar{\omega} : \bar{\omega} \le 0.16 \\ 0.245 : \bar{\omega} > 0.16 \end{cases} \tag{9b}$$

$$\phi_s = \begin{cases} 0 : \alpha^i \le \alpha_s + \Delta\alpha_s \\ \xi_{sp}\bar{\omega} : \alpha^i > \alpha_s + \Delta\alpha_s \end{cases} \tag{9c}$$

The dynamic overshoot of static $c_{l\max}$ for an airfoil describing oscillations in pitch, $\alpha = \alpha_0 + \Delta\theta \sin\omega t$, is sketched in Fig. 2. The figure shows c_l as a function of the separation-inducing angle of attack, (α^i), and not the instantaneous angle of attack, (α). That is, the figure shows only the $\Delta\alpha_s$ effects, and not the loop distortion due to time-lag effect,** nor the pitch-rate-induced apparent mass and camber effects.†† The airfoil stalls when

$$\alpha^i(t) = \alpha_s + \Delta\alpha_s \tag{10a}$$

$$\Delta\alpha_s = K_a\Delta\theta\bar{\omega}\cos\omega t \tag{10b}$$

§The "rolling leading edge" analogy used to describe this effect in Refs. 11 and 45 now has been tested experimentally. Johnson et al.[46] show that a rolling leading edge indeed delays the stall and that the delay is linearly dependent upon the leading-edge velocity, all in agreement with our postulations.

¶Although the details of the mathematical treatment are being debated,[28-31] no one has any quarrel with the physical justification of this flow concept.

**Although the time-lag effects are included when determining α^i for separation and reattachment, the full loop distorting time-lag effects are not shown until Fig 3.

††The pitch-rate-induced effects are very straightforward, as has been shown earlier[8] and is discussed in the Appendix.

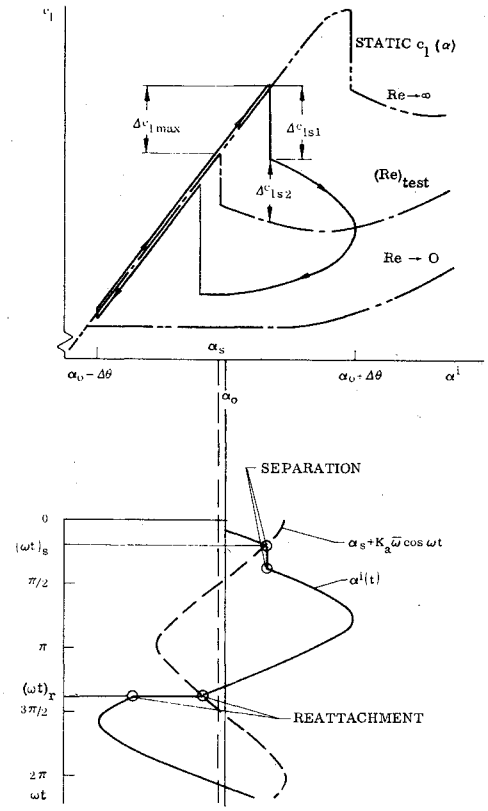

Fig. 2 Unsteady circulatory lift component as a function of effective angle of attack

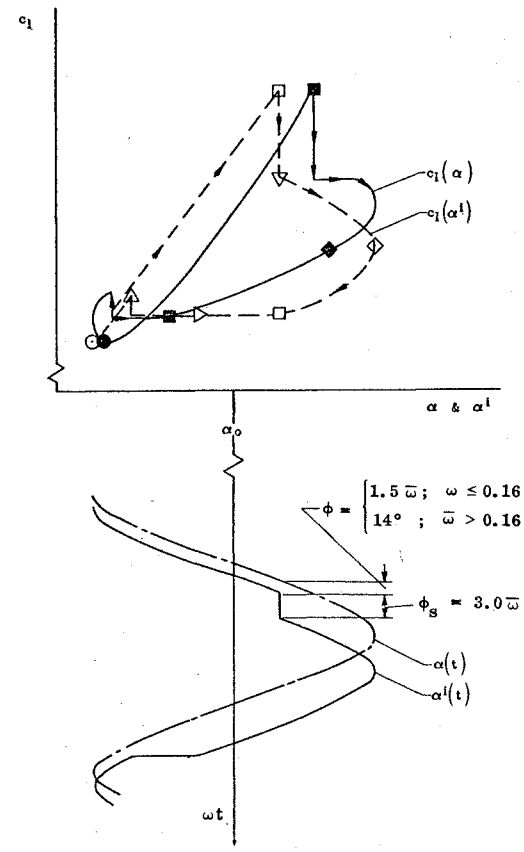

Fig. 3 Unsteady circulatory lift as a function of instantaneous angle of attack.

Stall resutls in a stepwise loss of lift (see Fig. 2).‡‡ On the "backstroke," reattachment occurs when Eq. (10) is satisfied again for $\omega t = (\omega t)_r$ (see Fig. 2). The c_l (α^i) stays at the minimum level until reattachment, a "backstroke" characteristic that is obtained even at zero frequency.[25] The "floor" for this minimum c_l is the zero Reynolds number limit, in analogy with the infinite Reynolds number limit for maximum lift.

When the time-lag effects are included, the c_l (α^i) loop in Fig. 2 is deformed as shown in Fig. 3 to give the lift variation with the instantaneous angle of attack, the c_l (α) loop.§§ The effect of the deep stall lag ϕ_s is large and becomes dominant at $\bar{\omega} > 0.16$, when the Karman-Sears wake lag has reached its saturation limit $\phi = 14°$. It is shown in Refs. 9 and 11 how the use of the dynamic flow concepts just discussed produces good prediction of the negative aerodynamic damping measured by Liiva et al. [23]

Recent Dynamic Stall Investigations

Since the time of the analysis reported in Ref. 9, numerous dynamic stall investigations have been performed. The results of investigations that have been detailed enough to provide new information about dynamic stall are analyzed to determine to what extent the basic flow concepts used in our engineering analysis[8,9,11] have to be changed or modified.

Numerical Results

A thorough numerical investigation of unsteady turbulent boundary layers has been performed by Scruggs et al. from which results for a NACA 0012 airfoil recently were presented.[16] They determined numerically how the delay of flow reversal at the midchord point depends on pitch rate and Reynolds number (Fig. 4). They show that the stall sensitivity to pitch rate decreases with increasing Reynolds number, in agreement with our postulation[8,9,11,24] that there is an equivalence between boundary-layer improvements due to dynamic effects and Reynolds number increase. That the "plateauing in Fig. 4 occurs at $(c\dot{\alpha}/U_\infty)$ values considerably beyond $c\dot{\alpha}/U_\infty = 0.02$ probably is because the theory is for incompressible flow, whereas the test data giving the 0.02 value are for leading-edge separation in compressible flow. Already at $M_\infty = 0.1$ the leading-edge peak velocity reaches $M_e = 0.4$ at stall.[9,24]

How the α-delay of the flow reversal point determined numerically[16] varies with chordwise position is shown in Fig. 5. Also shown is the estimate from our engineering analysis.[9,11] For separation well downstream of the leading edge, there is in addition to the inviscid flow circulation delay $\Delta\alpha_w$ also a convective time-lag effect $\Delta\alpha_c$ caused by the finite time required to convect upstream pressure gradient effects down through the boundary layer to the separation point. Using the convective velocity ratio $\bar{U}/U_e \approx 0.8$, measured by Kistler and Chen[33] for subsonic speeds, $\Delta\alpha_c$ can be approximated as[9,11]

$$\Delta\alpha_c + 1.25\xi_s c\dot{\alpha}/U_\infty \qquad (11)$$

This was the value used in Ref. 34 to reconstruct the "anomalous" effects of free boundary-layer transition on an oscillating airfoil.[35] The transition effects illustrated trailing edge separation as far as phase lag effects are concerned. Thus, according to our engineering analysis,[8,9,11] the total delay of separation well downstream of the leading edge obtained from Eqs. (1) and (11) is as follows

$$\Delta\alpha_w + \Delta\alpha_c = (1.5 + 1.25\xi_s)c\dot{\alpha}/U_\infty \qquad (12)$$

‡‡The transient effect of the "spilled leading edge" vortex has (so far) been neglected in our engineering analysis[8,9,11] When considering the moment characteristics and the associated dynamic-stall-induced negative aerodynamic damping, this transient does not have a significant effect as long as the frequencies are not high. At higher frequencies, however, this transient has to be included, together with other high-frequency flow phenomena.

§§Still without inclusion of pitch-rate-induced apparent mass and camber effects.

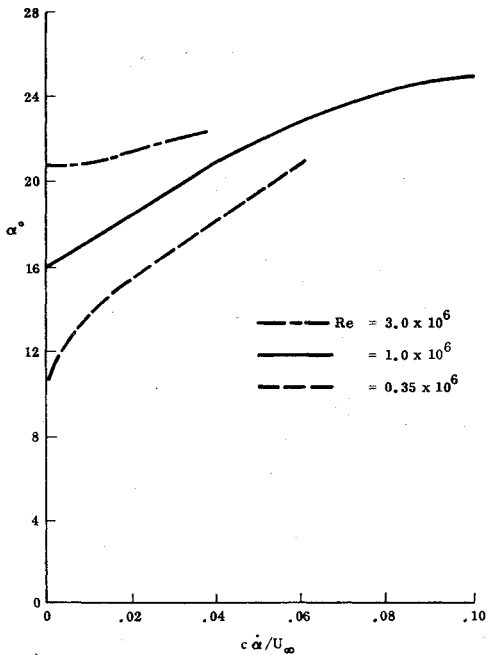

Fig. 4 Combined effect of Reynolds number and pitch rate on flow reversal.[16]

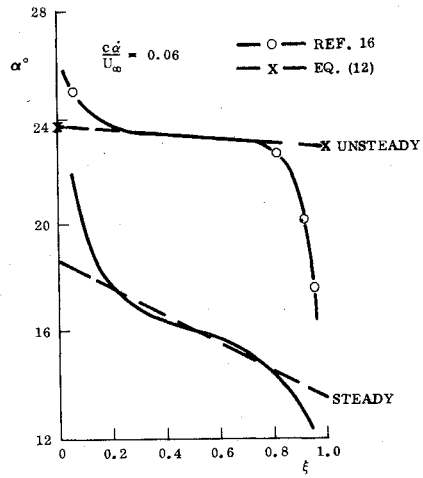

Fig. 5 Computed α-delay of flow reversal at different chordwise locations.

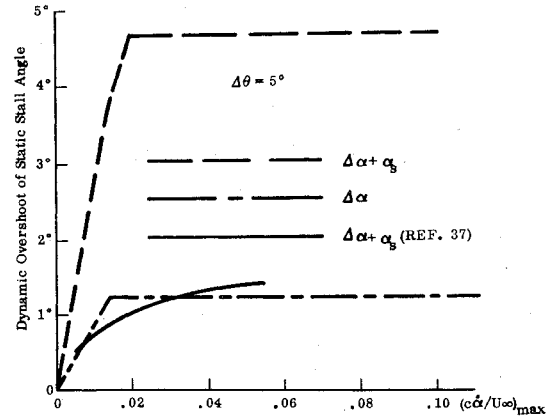

Fig. 6 Computed dynamic stall delay as a function of oscillatory frequency and amplitude.

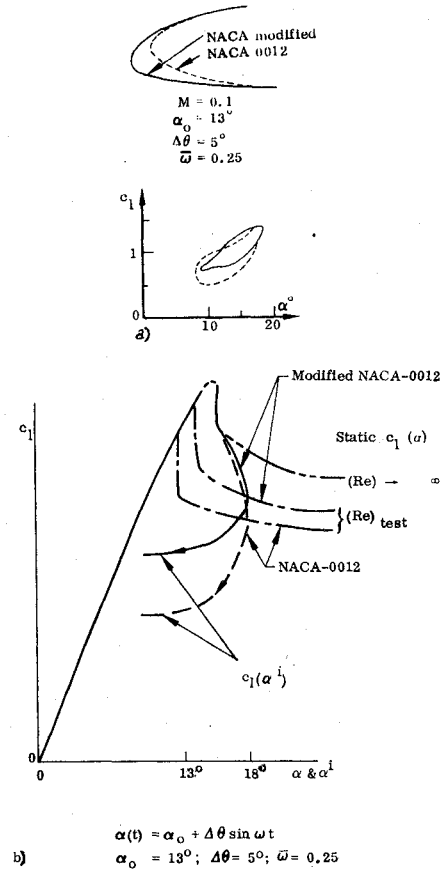

Fig. 7 Effect of leading edge droop on dynamic stall. a) Philippe's results. b) $c_l(t)=f(\alpha^i)$.

It can be seen that the results given by Eq. (12) agree remarkably well with the "exact" numerical computations. For simplicity, the static characteristics were approximated by straight lines when applying Eq. (12), neglecting the details near leading and trailing edges. These results support our hypothesis in Ref. 34 that the transition behaves dynamically very similarly to turbulent trailing-edge separation, a similarity also postulated by Kline,[36] and that, consequently, dynamic trailing-edge separation can be described by our simple engineering analysis.[8,9,11] The same conclusion has been reached by Lang.[37] For leading-edge stall, $\xi_s \to 0$, and $\Delta\alpha_c$ can be neglected.

Another extensive numerical study has been performed by Lang.[37] His numerical results for the delay of leading-edge stall are shown in Fig. 6. Also shown are the time lag $\Delta\alpha$ and the overshoot contributions $\Delta\alpha_s$ given by our engineering analysis[9,11] in which the $\Delta\alpha_s$ contribution is based on dynamic experimental data. It can be seen that the numerical results account for little more than the pure time-lag effect $\Delta\alpha$. This also is true for the results obtained by Scruggs et al.[16] when compared to measured dynamic delay of leading-edge stall. That is, no theoretical prediction presently is possible of the full viscous effects. Lang also quotes results reported by Fung[38] which give $\Delta c_{l\,\max} = 21.7\, c\dot{\alpha}/U_\infty$. For $c_{l_\alpha} = 2\pi$, this gives the value $K_a = 3.5$, which compares well with the value $K_a = 3.0$ used in our analysis[9,11] for $\xi_{CG} = 0.25$.

Experimental Results

Results obtained by Phillippe[39] illustrate the effect of static characteristics on the dynamic loops (see Fig. 7). Modifying a NACA-0012 airfoil by drooping the leading edge improves the static stall characteristics,[27,41] as is sketched in Fig. 7. With $\Delta\theta = 5°$ and $\bar{\omega} = 0.25$, the maximum pitch rate is $|c\dot{\alpha}/U_\infty| = 0.22$, and the infinite Reynolds number limit, which is the same for both airfoils, is reached. However, since leading-edge droop raises the static lift curve, the undershoot occurs

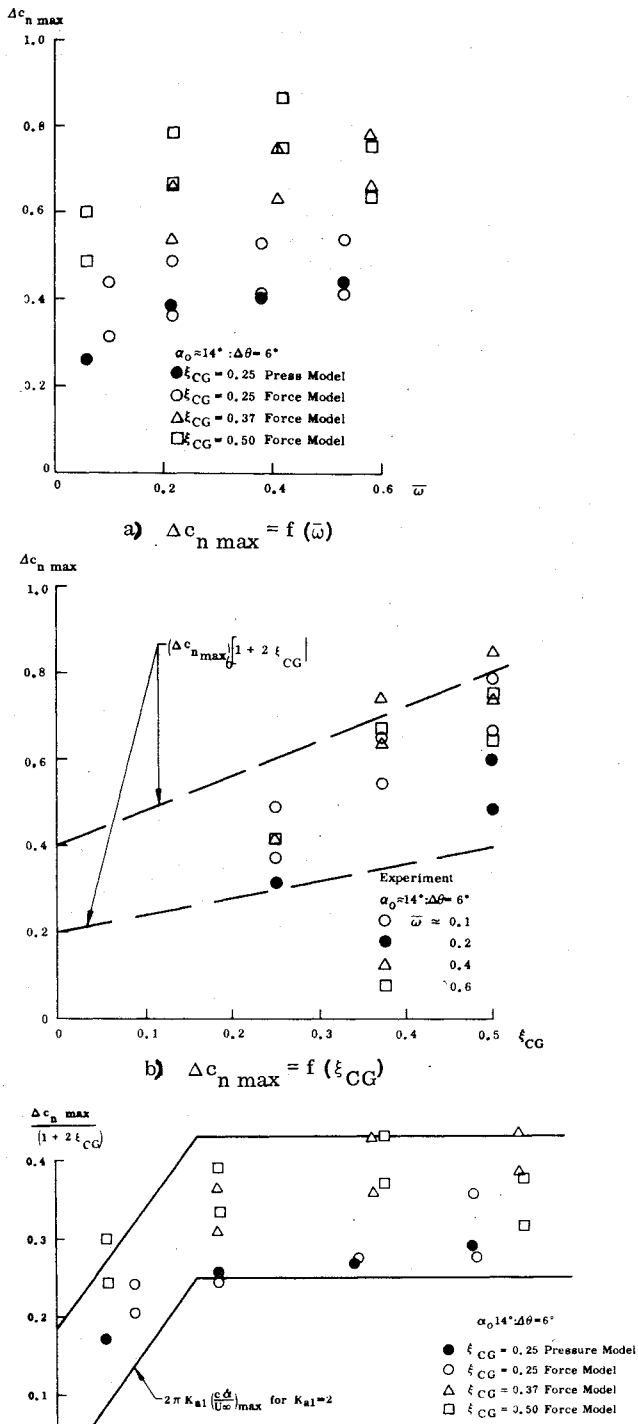

Fig. 8 Effect of oscillation center on dynamic stall overshoot[20].

from a higher static level, and the loop does not reach as low a c_l minimum as it does for the unmodified airfoil. Philippe's data illustrate how raising the static lift curve alters the dynamic lift loops. The effect of increasing Reynolds number is similar to that of leading-edge droop. It also raises the static lift curve, including static $c_{l\max}$ and deep stall lift,[21,16] and will result in a similar alteration of the dynamic loops.

Windsor's experiment[20] tends to support the existence of the "leading-edge jet" effect. It shows a definite influence of oscillation center ξ_{CG} on the dynamic overshoot of static $c_{l\max}$ (Fig. 8). When the results are plotted vs ξ_{CG} (Fig. 8b), the

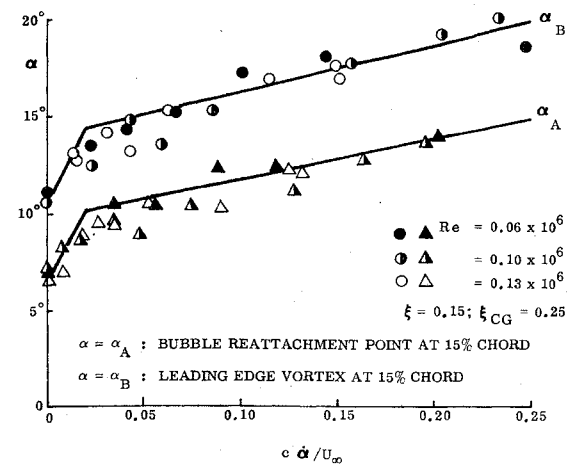

Fig. 9 Measured separation delay for different rate α-ramps.[42]

relationship $K_{a2} \approx 2K_{a1}$ in Eq. (6) is indicated. Normalizing the data using this ξ_{CG} dependence gives the results shown in Fig. 8c. The data seem to support the postulation made in Refs. 9 and 11 that the dynamic improvement effects have reached the saturation level, the infinite Reynolds number limit, at $|\dot{\alpha}c/U_\infty| > 0.02$.¶¶

Isogai's experiment[41,42] also tends to support this concept of $\Delta\alpha_s$ saturation at $c\dot{\alpha}/U_\infty > 0.02$ (see Fig. 9).*** The high pitch rate data have been fitted by straight lines, and the slope increase due to the $\Delta\alpha_s$ effect has been added for $c\dot{\alpha}/U_\infty < 0.02$ (using $K_a = 3$).

The most convincing prof of the existence of the "leading-edge jet" effect (or some other mechanism with similar characteristics) is provideed by the oscillatory plunging data obtained for an airfoil in the stall region by Liiva et al.[23] (Fig. 10). To our knowledge, no one has been able to explain how the negative aerodynamic damping is generated (Fig. 10a). As was discussed in Ref. 43, regular time-lag and pitch-rate induced effects can affect only the $\ddot{z}$ term and cannot contribute any to the damping, the $\dot{z}$ term. It will be shown how the loop reversal (Fig. 10b), which causes the negative aerodynamic damping, can be generated by the $\Delta\alpha_{s2}$ effect [Eq. (5); see Fig. 10c].

During the plunging upstroke, α' is negative, whereas both $\Delta\alpha_{s1}$ [Eq. (3)] and $\Delta\alpha_{s2}$ [Eq. (5)] are positive. For the test parameters in Fig. 10c, one obtains $\Delta\alpha_{s1}^0 = 0.33 \sin\omega t$ and $\Delta\alpha_{s2}^0 = 4.8 \cos\omega t$, with $K_{a1} = 2$, $K_{a2} = 4$. That is, the "leading-edge jet" effect $\Delta\alpha_{s2}$ is dominating. It is positive but decreasing during the upstroke and causes the airfoil to stall near the end of the upstroke. Reattachment occurs near the end of the downstroke. Thus, it is the "leading-edge jet" effect $\Delta\alpha_{s2}$ that generates the loop reversal responsible for the measured negative aerodynamic damping.

Conclusions

A second look at our engineering analysis[8,9,11] in light of recent numerical and experimental results has shown the following:

1) The concept of equivalence between boundary-layer improvement due to pitch-rate-induced effects and increasing Reynolds number is supported by available numerical and experimental results.

2) The existence of the postulated two different mechanisms for dynamic boundary-layer improvement is indicated by oscillatory stall data for different oscillation centers and by

¶¶The zero offset is indicative of tunnel side-wall boundary-layer interaction and resulting corner separation.[5] This also reduces the average lift as measured by a balance relative to that measured by the pressures at midspan.[20]

***α_A and α_B are the "angular times" at which large changes took place in the unsteady pressure gradient at $\xi = 0.15$.

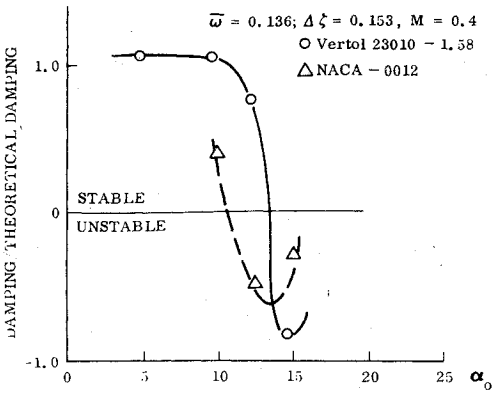

a) Damping in Plunge

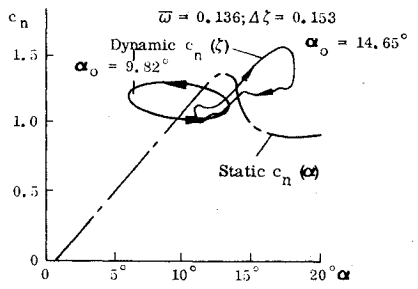

b) Plunging loops of Vertol 23010-158 at M = 0.4

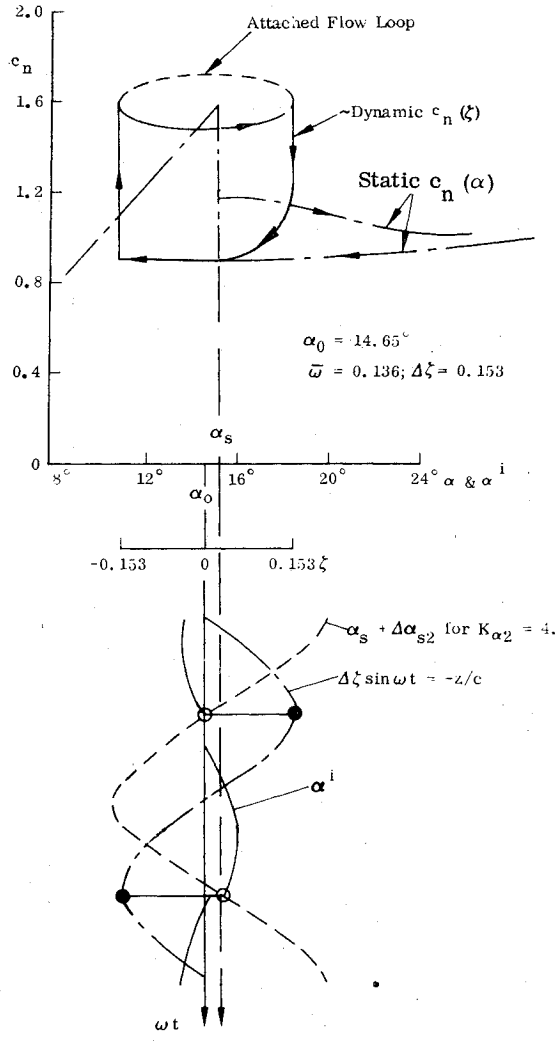

c) Construction of plunging loop

Fig. 10 Plunging-induced negative aerodynamic damping.[23]

measured negative damping for plunging oscillations in the stall region.

Appendix: Inviscid Dynamic Overshoot of Static Stall

That Carta's dynamic stall treatment is equivalent to our substall treatment can be shown very simply. Carta's expression for the lift is as follows [44]

$$c_l/2\pi = C(k)\alpha^* + C(k)\,\tfrac{1}{2}(\tfrac{1}{2}-a)\,(c\dot{\alpha}^*/U_\infty) + \tfrac{1}{4}(c\,\dot{\alpha}^*/U_\infty) - (a/8)\,(c^2\ddot{\alpha}/U_\infty^2) \quad \text{(A1)}$$

where

$$C(k) = F + iG,\quad a = 2\xi_{CG} - 1$$

$$\alpha^* = |\alpha| \exp(i\omega t)$$

The engineering analysis of Ref. 8 gives the following expression for c_l

$$[c_l(t) - c_l)_{\alpha_o})]/c_{l\alpha} = C(k)\theta^* + C(k) \cdot (c_{l\dot{\alpha}}/c_{l\alpha})\,(c\dot{\theta}^*/U_\infty) + [\tfrac{1}{2} - \xi_{CG} \cdot (c_{l\dot{\theta}})_{AM}/c_{l\alpha}]\,(c\dot{\theta}^*/U_\infty) + (c_{l\ddot{\theta}})_{AM} \cdot (c^2\ddot{\theta}^*/U_\infty^2) \quad \text{A2)}$$

Thin airfoil theory[39] gives $c_{l\alpha} = 2\pi$, $c_{l\dot{\alpha}}/c_{l\alpha} = (c_{l\dot{\theta}})_{AM}/c_{l\alpha} = \frac{1}{4}$, and $c_{l\ddot{\theta}_{AM}}/c_{l\alpha} = (\frac{1}{4}\ \frac{1}{2} - \xi_{CG})$. With $\xi_{CG} = (a+1)/2$, the right-hand side of Eq. (23) is identical (term by term) with the right-hand side of Eq. (22).†††

Carta recently has presented a note[13] that very convincingly argues that the large dynamic overshoot of static $c_{l\max}$ could be caused by the beneficial effects of the unsteady pressure gradient lag. Equation (2) in Ref. 13 can be recast in the following form (changing Carta's Cp to the lift-producing pressure differential ΔC_p)

$$\Delta C_p^*/4[(1-X)/(1+X)]^{\frac{1}{2}} = C(k)\alpha^* + C(k) \cdot \tfrac{1}{2}(\tfrac{1}{2}-a)\,(c\,\dot{\alpha}^*/U_\infty) + (X+\tfrac{3}{4})(c\,\dot{\alpha}^*/U_\infty) + \tfrac{1}{4}[(X/2)-a]\,(X+1)\,(c^2\ddot{\alpha}^*/U_\infty^2) \quad \text{(A3)}$$

where

$$\Delta C_p^* = |\Delta C_p| \exp(i\omega t)$$

Integration of Eq. (A3) gives Eq. (A1) (see Ref. 44). Thus, Carta's "additional lift" on the aft portion of the airfoil is simply the contribution from pitch-rate-induced camber and apparent mass effects which is negligibly small compared to the measured dynamic overshoot of static stall (see Fig. 1).

References

[1] Halfman, R.L., Johnson, H.C., and Haley, S.M., "Evaluation of High-Angle-of-Attack Aerodynamic Derivative Data and Stall-Flutter Prediction Techniques," NACA TN 2533, 1951.

[2] Liiva, J., "Unsteady Aerodynamic and Stall Effects on Helicopter Rotor Blade Airfoil Sections," *Journal of Aircraft,* Vol. 6, Jan.-Feb. 1969, pp. 46-51.

[3] Ham, N.D. and Garelick, M.S., "Dynamic Stall Considerations in Helicopter Rotors," *American Helicopter Society Journal,* Vol. 13, April 1968, pp. 44-55.

[4] Carta, F.O., "Unsteady Normal Force on an Airfoil in a Periodically Stalled Inlet Flow," *Journal of Aircraft,* Vol. 4, Sept.-Oct. 1967, pp. 416-421.

††† $\alpha^* = \theta^*$ for $\alpha_0 = 0$.

[5]Ericsson, L.E. and Reding, J.P., "Dynamic Stall Simulation Problems," *Journal of Aircraft,* Vol. 8, July 1971, pp. 579-583.

[6]Moss, G.F. and Murdin, P.M., "Two-Dimensional Low-Speed Tunnel Tests on the NACA 0012 Section Including Measurements Made During Pitch Oscillation at the Stall," Aeronautical Research Council, Great Britain, CP 1145, 1971.

[7]Gregory, N., Quincey, V.G., O'Reilly, C.L., and Hall, D.J., "Progress Report on Observations of Three-Dimensional Flow Patterns Obtained During Stall Development on Airfoils, and the Problem of Measuring Two-Dimensional Characteristics," Aeronautical Research Council, Great Britain; CP 1146; also Aero. Rept. 1309, National Physical Laboratory, 1969.

[8]Ericsson, L.E. and Reding, J.P., "Unsteady Airfoil Stall, Review and Extension," *Journal of Aircraft,* Vol. 8, Aug. 1971, pp. 609-616.

[9]Ericsson, L.E. and Reding, J.P., "Unsteady Airfoil Stall, Review and Extension," *Journal of Aircraft,* Vol. 8, Aug. 1971, pp. 609-616.

[9]Ericsson, L.E. and Reding, J.P., "Unsteady Airfoil Stall and Stall Flutter," NASA CR-111906, June 1971.

[10]von Karman, T. and Sears, W.R., "Airfoil Theory for Non-Uniform Motion," *Journal of the Aeronautical Sciences,* Aug. 1938, pp. 379-390.

[11]Ericsson, L.E. and Reding, J.P., "Analytic Prediction of Dynamic Stall Characteristics," AIAA Paper 72-682, Boston, Mass., June 1972.

[12]Harper, P.W. and Flanagan, R.E., "The Effect of Rate of Change of Angle of Attack on the Maximum Lift of a Small Model," NACA TN 2061, 1949.

[13]Carta, F.O., "Effect of Unsteady Pressure Gradient Reduction on Dynamic Stall Delay," *Journal of Aircraft,* Vol. 8, Oct. 1971, pp. 839-841.

[14]Shamroth, S.J. and McDonald, H., "Application of Time-Dependent Boundary-Layer Analysis to the Problem of Dynamic Stall," *Journal of Applied Mechanics,* Sept. 1972, pp. 823-825.

[15]Schlichting, H., *Boundary Layer Theory,* translated by J. Kestin, McGraw Hill, New York, 1955, pp. 206-214.

[16]Scruggs, R.M., Nash, J.F., and Singleton, R.E., "Analysis of Flow-Reversal Delay for a Pitching Foil," AIAA Paper 74-183, Washington, D.C., Jan. 1974.

[17]Hurley, D.G. and Ward, G.F., "Experiments on the Effects of Air Jets and Surface Roughness on the Boundary Layer Near the Nose of an NACA 64A006 Airfoil," Aeronautical Research Laboratories, Melbourne, Australia, Aero Note 128, Sept. 1953.

[18]Wallis, R.A., "Boundary Layer Transition at the Leading Edge of Thin Wings and its Effect on General Nose Separation," *Advances in Aeronautical Sciences, Proceedings of the Second International Congress in the Aeronautical Sciences,* Sept. 12-16, Zurich, pp. 161-184.

[19]Wallis, R.A., "The Turbulent Boundary Layer on the Articulated Nose of a Thin Wing Provided with Air Jets," Aeronautical Research Laboratories, Melbourne, Australia, Aero Note 141, Oct. 1954.

[20]Windsor, R.I., "Measurements of Aerodynamic Forces on an Oscillating Airfoil," TR 69-98, March 1970, U.S. Army Aviation Labs., Fort Eustis, Va.

[21]Jacobs, E.N. and Sherman, A., "Airfoil Section Characteristics as Affected by Variations in the Reynolds Number," NACA TR 586, 1937.

[22]Abbot, I.H., Von Doenhoff, A.E., and Stivers, L.S., "Summary of Airfoil Data," NACA TR 824, 1945.

[23]Liiva, J., Davenport, F.J., Gray, L., and Walton, I.C., "Two-Dimensional Tests of Airfoils Oscillating Near Stall," TR 68-13, April 1968, U.S. Army Aviation Labs, Fort Eustis, Va.

[24]Ericsson, L.E. and Reding, J.P., "Stall Flutter Analysis," *Journal of Aircraft,* Vol. 10, Jan. 1973, pp. 5-13.

[25]Critzos, C.C., Heyson, H.H., and Boswinkle, R.W., Jr., "Aerodynamic Characteristics of NACA-0012 Airfoil Section at Angles of Attack from 0 to 180°," NACA TN 336, 1955.

[26]Ericsson, L.E. and Reding, J.P., "Unsteady Airfoil Stall," CR 66787, 1969.

[27]Moore, F.K., "On the Separation of the Unsteady Laminr Boundary Layer," *IUTAM Symposium on Boundary Layer Research,* Aug. 26-29, 1957, Freiburg, pp. 296-311.

[28]Sears, W.R. and Telionis, D.P., "Unsteady Boundary-Layer Separation," *Proceedings of IUTAM Symposium on Unsteady Boundary Layers,* Vol. 1, May 1971, Quebec, pp. 404-447.

[29]Buckmaster, J., "On Kaplun's Method for Studying Separation," *Proceedings of IUTAM Symposium on Unsteady Boundary Layers,* Vol. 1, May 1971, pp. 462-475.

[30]Sears, W.R. and Telionis, D.P., "Comments on Paper by J. Buckmaster," *Proceedings of IUTAM Symposium on Unsteady Boundary Layers,* Vol. 1, May 1971, Quebec, pp. 476-477.

[31]Buckmaster, J., "Author's Reply to Comments by Professor Sears and Dr. Telionis," *Proceedings of IUTAM Symposium on Unsteady Boundary Layers,* Vol. 1, May 1971, Quebec, pp. 477-480.

[32]Brady, W.G. and Ludwig, G.R., "Research on Unsteady Stall of Axial Flow Compressors," Cornell Aeronautical Laboratories, Buffalo, N.Y., Rept. AM-1762-S-4, Nov. 1963.

[33]Kistler, A.L. and Chen, W.S., "The Fluctuating Pressure Field in a Subsonic Turbulent Boundary Layer," Jet Propulsion Laboratory, Pasadena, Calif., TR 32-277, Aug. 1962.

[34]Ericsson, L.E. and Reding, J.P., "Dynamic Stall of Helicopter Blades," *American Helicopter Society Journal,* Vol. 17, Jan. 1972, pp. 11-19.

[35]Greidanus, J.H., van de Vooren, A.I., and Bergh, H., "Experimental Investigation of the Aerodynamic Characteristics of an Oscillating Wing with Fixed Axis of Rotation," Rept. F101, Jan. 1952, National Aerospace Laboratory, Amsterdam, Holland.

[36]Kline, S.J., "Some New Concepts of the Mechanics of Stall in Turbulent Boundary Layers," *Journal of the Aeronautical Sciences,* Vol. 24, June 1957, pp. 470-471.

[37]Lang, J.D., "On Predicting Leading-Edge Bubble Bursting on an Airfoil in Unsteady Incompressible Flow," Cranfield Memo 109, April 1973.

[38]Fung, Y.C., *An Introduction to the Theory of Aeroelasticity,* Dover, N.Y., 1968.

[39]Philippe, J.J., "Le Decrochage Instationnaire d'un Profil," ONERA, TP 936, 1968.

[40]Kelly, J.A., "Effect of Modifications to the Leading-Edge Region on the Stalling Characteristics of the NACA 63-012 Airfoil Section," NACA TN 2228, 1950.

[41]Ham, N.D., "Some Recent MIT Research on Dynamic Stall," *Journal of Aircraft,* Vol. 9, May 1972, pp. 378-379.

[42]Isogai, K., "An Experimental Study on the Unsteady Behavior of a Short Bubble on an Airfoil During Dynamic Stall with Special Reference to the Mechanism of the Stall Overshoot Effect," MIT, Aeroelastic and Structures Research Lab., Cambridge, Mass., TR 130-2, June 1970.

[43]Ericsson, L.E., "Dynamic Effects of Shock-Induced Flow Separation," *Journal of Aircraft,* Vol. 12, Feb. 1975, pp. 86-92.

[44]Arcidiacono, P.J., Carta, F.O., Casellini, L.M., and Elman, H.L., *"Investigation of Helicopter Control Loads Induced by Stall Flutter,"* U.S. Army Aviation Material Labs., Fort Eustis, Va., TR 70-2, March 1970.

[45]Ericsson, L.E. and Reding, J.P., "Dynamic Stall Analysis in Light of Recent Numerical and Experimental Results," AIAA Paper 75-26, Pasadena, Calif., Jan. 1975.

[46]Johnson, W.S., Tennant, J.S., and Stamps, R.E., "Leading-Edge Rotating Cylinder for Boundary-Layer Control on Lifting Surfaces," *Journal of Hydronautics,* Vol. 9, April 1975, pp. 76-78.